# Chapter 5

# Analysis of Facilitated Oxygen Transport through the Polymeric Cobaltporphyrin Membrane with a Fluctuation Concentration Model

## 5.1 Introduction

In previous chapter, the author described that the very efficient facilitated oxygen transport in the polymeric simple and planar cobaltporphyrin thin membrane improved both the selectivity and flux of the oxygen. The characteristics of this membrane are (i) extraordinary large oxygen-dissociate rate constant ($10^6$ $s^{-1}$) of the simple and planar porphyrin, (ii) high cobaltporphyrin-loading (42wt%) concentration, and (iii) a sub-micron thickness (85nm) to obtain high flux. Theoretical analysis of the effect of these characteristics to the facilitated oxygen transport is desired.

One of the typical models to explain the mechanism of facilitated transport, Paul and Koros[1] and Petropoulos[2] proposed and established a dual-mode transport theory to explain the transport behavior of condensable gases such as carbon dioxide in glassy polymer. This model has been commonly employed, because it is conceptually analogous to the mass transport in a facilitated transport membrane with fixed site carriers and it has a mathematical simplicity. However, it does not provide for the dependency of the permeability of the matrix, the exchange rate of solute between carrier and matrix and the membrane thickness.

Recently, Kang et al. proposed that a simple mathematical model for the facilitated mass transport with a fixed site carrier membrane.[3-5] This model was derived by assuming an instantaneous, microscopic concentration (activity) fluctuation in the membrane. The concentration fluctuation, developed due to the reversible chemical reaction between carrier and solute, could cause the higher chemical potential gradient and the facilitated transport (shown in Figure 5-1). For mathematical formulation, the fluctuated concentration profile was assumed to be a sinusoidal, which is analogous to an alternating voltage in electric circuit. An analogy was employed between the mass transfer for the facilitated transport with fixed site carrier membrane and the electron transfer in a single parallel resistor-capacitor (RC) circuit.

In this chapter, the author reports the effect of (a) membrane thickness and (b) equilibrium constant of the oxygen-binding on the facilitated oxygen transport through the cobalt tetraphenylporphyrin membrane. Concentration fluctuation model was also applied to analyze this facilitated oxygen transport.

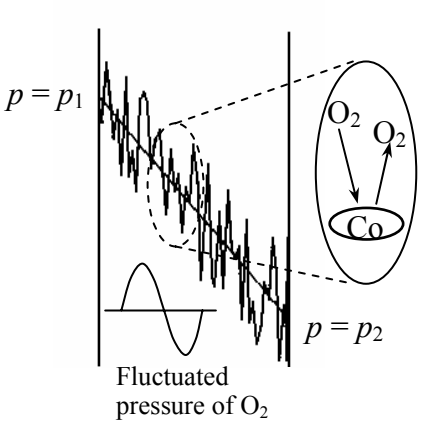


**Figure 5-1**. A fluctuated pressure profile in a facilitated transport membrane with fixed site carrier at steady state.

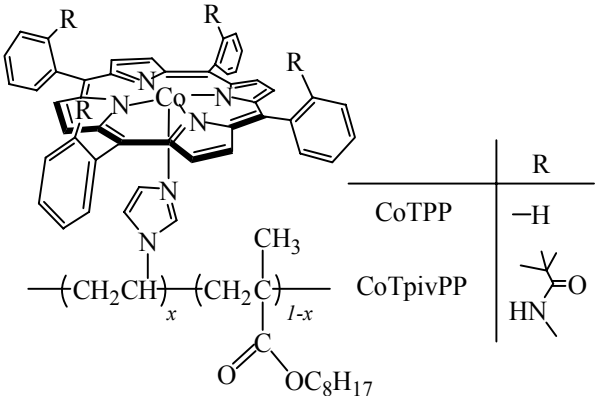


**Scheme**

## 5.2 Experimental

### 5.2.1 Material

Cobalt-5,10,15,20-tetraphenylporphrin (CoTPP) was purchased from Aldrich Co., Ltd and used as received. Cobalt meso-α,α,α,α-tetrakis(*o*-pivalamidophenyl)porphyrin (CoTpivPP) was synthesized as in the literature.[6] (Poly(octyl methacrylate-*co*-1-vinylimidazole) (OIm) was prepared by radical polymerization of octyl methacrylate and 1-vinylimidazole with azobisisobutylonitrile, and used as a polymer-ligand (content of the vinylimidazolyl residue = 30 mol% ; $[\eta]$ = 0.64 g/dl, toluene, 30°C by elemental analysis and viscometric measurement, respectively).

### 5.2.2 Membrane Preparation

Tetrahydrofurane solution of the CoTPP-OIm complex were mixed, and the solution was carefully cast on a polyacrylonitrile porous support membrane (GMT

Membrantechnik, BRD) with the coating bar (R K Print Coat Instruments Ltd.) under an oxygen-free atmosphere Then the membranes were followed by drying in vacuo, to yield a transparent, orange composite membrane with a thickness of 80-90 nanometer of the CoTPP-OIm layer. The series of CoTPP-OIm membranes were prepared at a constant CoTPP concentration (42 wt%) in the membranes. Same morphology for these membranes were confirmed.[7]

### 5.2.3 Permeation Measurement

The permeation properties of the CoTPP-OIm membrane were investigated with an oxygen or nitrogen at room temperature. The feed pressure range was 1-78kPa (gauge pressure), while the permeate-side pressure was atmospheric. Volumetric gas flow rates were measured with a soap-bubble flowmeter. A schematic diagram of gas permeation apparatus is shown in Figure 5-2. The membrane area exposed to the feed gas was 3.14cm$^2$. Experiments were carried out at high to low pressure; at each pressure at least 40 minutes have passed before getting the data point at steady state.

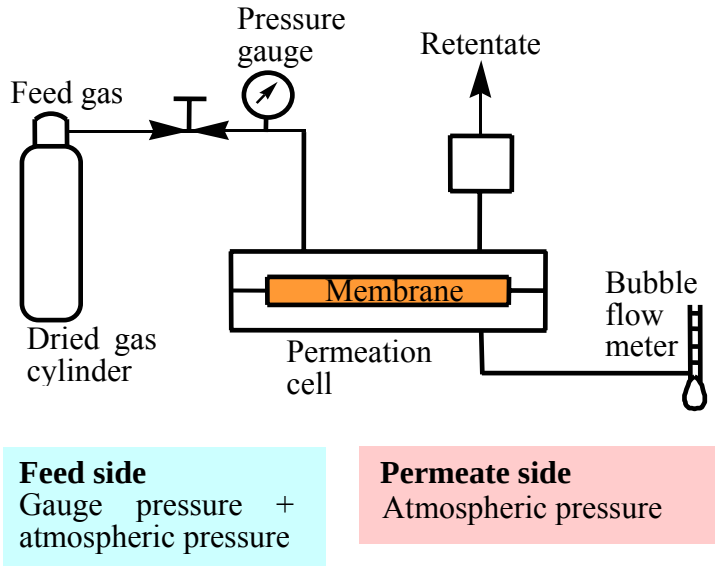


**Figure 5-2.** Apparatus for the permeability measurement

## 5.3 Theoretical Background

In a fixed site carrier membrane, reversible reaction between a carrier and penetrant causes the concentration fluctuation in the membrane. When the penetrant reacts with the carrier to make penetrant-carrier complex, the local penetrant concentration or pressure at that specific site will be decreased instantaneously from its average value. In other hand, it will be increased when the complex releases the penetrant into the matrix.

Therefore, the chemical potential of the penetrant will be increased owing to the concentration fluctuation. This fluctuated pressure $p$ is defined as $p = p_a + p_d \sin(\omega t)$, where $p_a$ is time-averaged pressure, thus $p_d$ shows the amplitude of the concentration fluctuation. The increased chemical potential will result in a higher driving force for mass transfer and read to the facilitated transport.

Based on above concepts and analogy between electron transfer in a single parallel RC circuits and mass transport in a fixed site carrier membrane, Kang et al proposed the following model to explain the facilitated transport in a fixed site carrier membrane (see the detail in ref. 3).

$$\frac{P_{O2}}{\overline{P}} = 1 + \left(\frac{p_d}{p_0}\right)\sqrt{n^2 + \left\{\frac{2\pi k_2 L^2 C_B^0}{\overline{P}}\frac{\ln(1+Kp_0)}{p_0}\right\}^2} \qquad (5\text{-}1)$$

Here, $P_{O2}$ and $\overline{P}$ are the permeabilities of penetrant in facilitated transport membrane and matrix ($P_{O2}$ of the inactive membrane), respectively, $p_d$ and $p_0$ are the pressure fluctuation and pressure at membrane surface, respectively, $n$ is the number of hypothetical layers representing the number of carrier molecules that a penetrant can meet in its diffusional pathway, $k_2$ and $K$ are the reverse reaction rate and reaction equilibrium constants between penetrant and carrier, respectively, $L$ is the membrane thickness, and $C_B^0$ is the initial carrier concentration loaded in the membrane.

When total carriers in a membrane are regarded as one capacitor (i.e. $n$=1) and its matrix as one resistor, Eq. 5-1 is reduced to a single RC circuit model as follows

$$\frac{P_{O2}}{\overline{P}} = 1 + \left(\frac{p_d}{p_0}\right)\left(\frac{2\pi k_2 L^2 C_B^0}{\overline{P}}\frac{\ln(1+Kp_0)}{p_0}\right) \qquad (5\text{-}2)$$

Since Eq. 5-3 is generally valid for normal experimental conditions

$$\left(\frac{2\pi k_2 L^2 C_B^0}{\overline{P}}\frac{\ln(1+Kp_0)}{p_0}\right)^2 \rangle\rangle\ 1 \qquad (5\text{-}3)$$

To correlate the permeability data in a facilitated transport membrane with fixed site carriers, $P_{O2}$, as a function of upstream pressure, $p_0$, six out of seven parameters should be determined a priori. The remaining parameter, $p_d$, can be estimated, using the measured permeability data, by a linear regression of Eq. 5-2.

In this experiment the apparatus shown Figure 5-2 is used as a permeability measurement. Through all the measurement, pure gas was applied to the upstream, so the pressure of permeate side is always maintained at 1atm. Considering of this ($p_0 = p_1 - p_2$), the modified model derived as below was applied to this facilitated transport.

$$F = \frac{P_{O2}}{\overline{P}} = 1 + \left( \frac{p_d}{p_1 - p_2} \right) \frac{2\pi k_2 L^2 C_B^0}{\overline{P}} \frac{1}{(p_1 - p_2)} \ln\left( \frac{1 + Kp_1}{1 + Kp_2} \right) \quad (5\text{-}4)$$

where, $p_1$ is upstream pressure and $p_2$ is downstream pressure.

For convenience, Eq. 5-4 was converted to a non-dimensional form as follows when $P = DS$ and $C_A^\infty = Sp_o$.

$$F = 1 + 2\pi\alpha_p \psi\lambda \ln(1 + \Delta) \quad (5\text{-}5)$$

Where, $\alpha_p$ is the extent of the pressure fluctuation (= $p_d/(p_1 - p_2)$), $\psi$ is the ratio of the time scales of diffusion to chemical reaction (= $k_2L_2/D$), $\gamma$ is the ratio of the total carrier concentration to the solute solubility in matrix (= $C_B^0/C_A^\infty$), $\Delta$ is the combined driving force for facilitation (= $K(p_1 - p_2)$), $D$ is diffusion coefficient of solute through matrix, $S$ is Henry's law solubility coefficient of solute in matrix, and $C_A^\infty$ is concentration of solute in matrix. In these dimensionless parameters, $\psi$ is constant, thus $\psi$ and $p_d$ value, which is also constant, were chosen as the parameters for comparison.

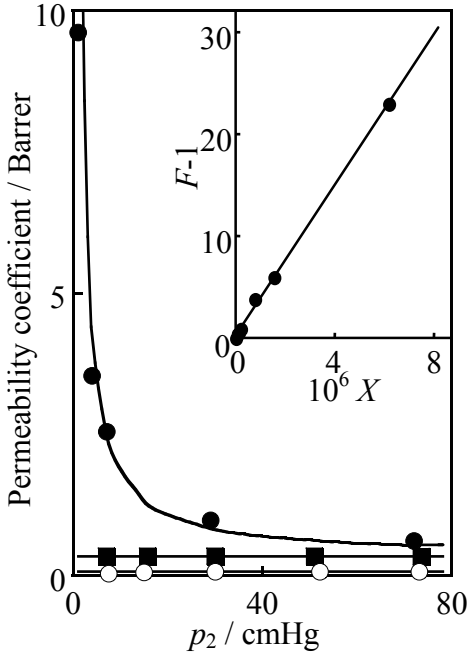


**Figure 5-3.** Plots of experimental data and theoretical prediction line of oxygen permeability through CoTPP-OIm membrane with 85nm thickness. Experimental data of oxygen(●), nitrogen(○), and oxygen for inactive membrane(■). Line: theoretical prediction according to Eq. 5-4. Inset: Plots of $F$-1 vs $\{1/(p_1\text{-}p_2)^2\}$ $(2\pi k_2 L^2 C_B{}^0/\overline{P})\ln\{(1+Kp_1)/(1+Kp_2)\}$ (= $X$) according to Eq. 5-4.

**Table 5-1**. Experimental results for and the parameters from the concentration fluctuation model

| Porphyrins | $L$ [a)] | $P_{N2}$ [b)] | $\alpha$ | $F$ | $10^6 p_d$ | $\psi$ |
|---|---|---|---|---|---|---|
| CoTPP (42wt%) | 85 | 7.9 | 123 | 28 | 23 | 7600 |
| | 120 | 8.7 | 102 | 26 | 7.2 | 14000 |
| | 160 | 8.1 | 103 | 24 | 3.7 | 26000 |
| | 230 | 8.5 | 123 | 29 | 1.6 | 55000 |
| CoTPP (20wt%) | 90 | 8.7 | 42 | 10 | 3.6 | 3800 |
| CoTpivPP (20wt%) | 87 | 20 | 7.0 | 6.7 | 3200 | 7.9 |

a) nm, b) Barrer

## 5.4 Effect of membrane thickness on the facilitated transport

The series of the CoTPP-OIm membrane with different membrane thickness were prepared and displayed to the permeation measurement. $L$ and the nitrogen permeability coefficient ($P_{N2}$) of these membranes were listed in Table 5-1. $P_{N2}$ were constant regardless of the membrane thickness, which indicates these membranes have almost the same morphology. The typical example of $P_{O2}$ for the series of the CoTPP-OIm membranes plotted by the oxygen pressure difference between upstream and downstream was shown in Figure 5-3. $P_{O2}$ is larger than $P_{N2}$ (see the Table 5-1) and steeply increased with a decrease in $p_0$. $P_{O2}$ for a control membrane composed of inactive Co(III)TPP membrane is not enhanced at low $p_0$, whereas $P_{O2}$ for the active membranes significantly increases. $P_{O2}$ increases to 9.6 Barrer (1 Barrer = $10^{-10}$ $cm^3$(STP) cm/ $cm^2$ s cmHg). The extremely high permselectivity ($\alpha = P_{O2} / P_{N2}$ at 77cmHg) and $F$ at 77cmHg were calculated and also listed in Table 5-1 and were almost independent of the membrane thickness.

## 5.5 Effect of equilibrium constant of the oxygen-binding on the facilitated transport

The facilitated or cobaltporphyrin-mediated transport was affected by the cobaltporphyrin species; i.e. oxygen-binding affinity and kinetic activity ascribed to the porphyrin structure. To consider the effect of the equilibrium constant of the oxygen-binding, the picket-fence cobalt porphyrin (CoTpivPP) was selected as the oxygen carrier with high oxygen-binding affinity. Figure 5-4 shows the $P_{O2}$ and $P_{N2}$ for

the CoTpivPP (CoTpivPP content = 20wt%). $P_{O2}$ for the CoTpivPP-OIm membrane is also larger than $P_{N2}$ and steeply increased with a decrease in $p_0$. $P_{O2}$ for a control membrane composed of inactive Co(III)TPP membrane is not enhanced at low $p_0$, whereas $P_{O2}$ for the active membranes significantly increases. $P_{O2}$ increases to 9.4 Barrer and α and $F$ at 77cmHg were listed in Table 5-1.

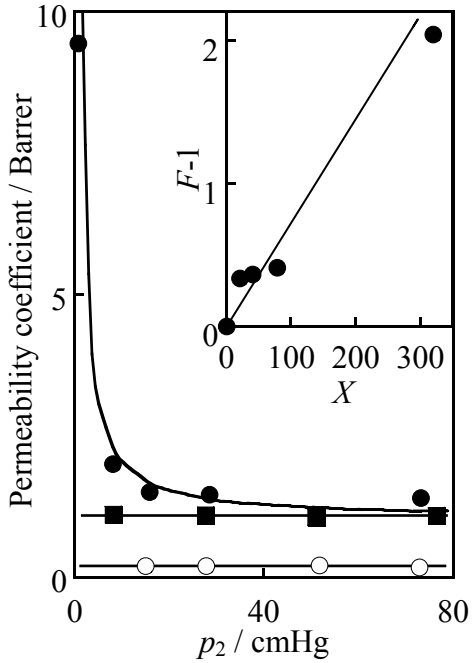


**Figure 5-4.** Plots of experimental data and theoretical prediction line of oxygen permeability through CoTpivPP-OIm membrane with 85nm thickness. Experimental data of oxygen(●), nitrogen(○), and oxygen for inactive membrane(■). Line: theoretical prediction according to Eq. 5-4. Inset: Plots of $F$-1 vs $\{1/(p_1-p_2)^2\}$ $(2\pi k_2 L^2 C_B^0/\bar{P})\ln\{(1+Kp_1)/(1+Kp_2)\}$ (= $X$) according to Eq. 5-4.

**Table 5-2**. Experimental results for the concentration fluctuation model

| Porphyrins | $10^4 C_B^{0a)}$ | $10^4 k_D^{b)}$ | $10^{-6} k_2^{c)}$ | $10^3 K^{d)}$ |
|---|---|---|---|---|
| CoTPP (42wt%) | 6.8 | 4.6 | 7.6 | 1.3 |
| CoTPP (20wt%) | 3.6 | 8.6 | 7.6 | 1.3 |
| CoTpivPP (20wt%) | 0.92 | 9.1 | 0.012 | 130 |

a) mol/cm$^3$, b) cm$^3$(STP)/cm$^3$ cmHg, c) 1/s, d) 1/cmHg.

Comparison with Figure 5-3 and 5-4, both $\alpha$ and $F$ of the CoTPP membrane were larger than that of CoTpivPP. These figures also indicates the pressure at which facilitated oxygen transport observed is affected by the equilibrium constant of

oxygen-binding reaction, that is, with larger $K$, more easily the carrier saturation occurs, which indicates facilitated oxygen transport observed at higher pressure. This result corresponds with our previous report.

## 5.6 Analysis of the facilitated oxygen transport with the concentration fluctuation model

The effect of the membrane thickness the oxygen facilitated transport was analyzed with the concentration fluctuation model. The experimental values, which were obtained spectroscopically[13] as listed in Table 5-2, were used as the parameters for this model. The plots of $F$-1 *vs* $(1/(p_1\text{-}p_2)^2)$ $(2\pi k_2 L^2 C_B^0/\bar{P})$ $\ln\{(1+Kp_1)/(1+Kp_2)\}$ $(= x)$ were shown in inset of the Figure 5-3 and linear relationship in obtained. The slope of this line was calculated to obtain $p_d$ value (as listed in Table 5-1). The theoretical prediction of the $P_{O2}$ is calculated from obtained $p_d$ and has good agreement with the experimental results shown in Figure 5-3. $p_d$ in Table 5-1 indicates the following; $p_d$ were increased with a decrease in membrane thickness. The experimentally obtained $p_d$ was increased with a decrease in membrane thickness. In this model, The pressure $p$ is defined as $p = p_a + p_d \sin(\omega t)$, where $p_a$ is time-averaged pressure, thus $p_d$ shows the amplitude of the concentration fluctuation. From the definition, $F$ should increase with membrane thickness and $p_d$ should be constant. But the calculated $p_d$ listed in Table 5-1 seems increase with a decrease in membrane thickness. That indicates the $p_d$ and $\psi$ seem to cancel each other because $F$ are almost constant regardless of the membrane thickness.

The line in Figure 5-4 supports the modified concentration fluctuation model was agreed with the experimental plots. The calculated parameters for these membranes are summarized in Table 5-1. Dr. Kang also reported the permeability predictions as varying parameter $K$ show that facilitation ability of fixed site carrier membranes increases as $K$, however, the experimental results show the inverse relationship between the reaction equilibrium constant and the facilitation ability.[9] For example, $K$ of CoTPP is smaller than that of CoTpivPP, but the $F$ is larger as shown in Table 5-1. This seems one of the limits of this concentration fluctuation model.

## References

1. D. R. Paul and W. J. Koros, *J. Polym. Sci., Polym. Phys. Ed.*, **27**, 177 (1976).
2. J. H. Petropoulos, *J. Polym. Sci., A-2*, **8**, 1797 (1970).
3. Y. S. Kang, J. H. Hong, J. Jang, U. Y. Kim, *J. Membr. Sci.*, **109**, 149 (1996).
4. J. H. Hong, Y. S. Kang, J. Jang, U. Y. Kim, *J. Membr. Sci.*, **109**, 159 (1996).

5. S. U. Hong, J. Won, H. C. Park, Y. S. Kang, *J. Membr. Sci.*, **163**, 103 (1999).
6. J. P. Collman, R. R. Gagne, C. A. Reed, J. R. Halbert, G. M. Lang, T. Robinson, *J. Am. Chem. Soc.*, **97**, 1427 (1995).
7. H. Shinohara, A. Nakao, H. Nishide, *Kobunshi Ronbunshu*, **59**(10), 655 (2002).
8. H. Shinohara, T. Arai, H. Nishide, *Macromol. Symp.*, **186**, 135 (2002).
9. H. Nishide, T. Suzuki, H. Kawakami, E. Tsuchida, *J. Phys. Chem.*, **98**(19), 5084 (1994).